# Supplementary Material

# Describing Autophagy via Analysis of Individual Organelles by Capillary Electrophoresis with Laser Induced Fluorescence Detection

*Chad P. Satori and Edgar A. Arriaga**

University of Minnesota Twin-Cities

Department of Chemistry, 207 Pleasant St. SE

Minneapolis MN 55455-0431

*Corresponding author

**Table of Contents**

## S-1. Fluorescence Confocal Microscopy

Preparation of cells for fluorescent confocal microscopy was done as previously described.[50] Briefly, LabTek 4 chambered coverslips were incubated with poly-L-lysine (100 μL) for 30 min. prior to cell culture to improve cellular attachment to the coverslip. Cells were treated with vinblastine, rapamycin, or both vinblastine and rapamycin. Cells were fixed with 4% v/v formaldehyde in water, then permeabilized with 10% v/v Triton X-100 in water, and finally incubated with 5% w/v BSA to reduce non-specific binding of antibodies.[50] Cells were then incubated with rabbit anti-LC3 antibody (1 μL in 250 μL; 2% w/v BSA in 1× PBS) overnight. Cells were then washed with 1× PBS three times for 5 minutes with PBS. Cells were then incubated with goat anti-rabbit AlexaFluor568 secondary antibody (1 μL in 250 μL; 2% w/v BSA in 1× PBS) for 1 hour. Cells were again washed with 1× PBS for 5 minutes three times to remove unbound antibody.

Images were acquired with an Olympus IX81 inverted microscope (Melville, NY) as previously described.[50] Data analysis of microscopy images was done with Simple PCI 5.3 (Compix Inc., Cranberry Township, PA) as previously described.[50] Colocalization was calculated between GFP-LC3 and anti-LC3 fluorescent signals using Equations S-1, S-2, S-3, and S-4.[51] The M2 coefficient confirmed the GFP-transfected protein was LC3 (Table S-1). High correlation values from four different correlation examinations (R, r, ICQ, and M2) were determined when comparing GFP and AlexaFluor568 (See Supplementary Information, Table S-1). GFP-labeled organelles were observed in all samples with more intense organelles appearing in the vinblastine-treated samples (Figure S-1).

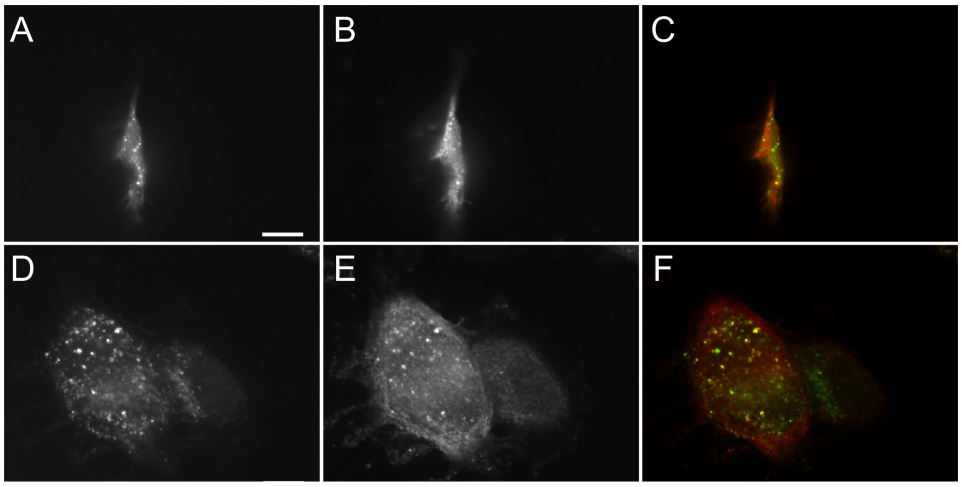


**Figure S-1.** Exemplary fluorescence confocal microscopy of two different vinblastine-treated L6 cells expressing GFP-LC3. Green fluorescence is from GFP-LC3 and red fluorescence is from the secondary antibody labeled with AlexaFluor 586. (A) AlexaFluor 568 fluorescence of vinblastine-treated cell. (B) GFP fluorescence of vinblastine-treated cell. (C) Overlay of (A) and (B). (D) AlexaFluor 568 fluorescence of vinblastine-treated cell. (E) GFP fluorescence of vinblastine-treated cell. (F) Overlay of (D) and (E). Scale bar = 10 μm.

**S-2. Microscopy Correlation and Colocalization Equations**

The background level was determined using five regions of interest (ROIs) of the extracellular space. The average of the pixel values of the ROI fluorescence ($Ave_{ROI}$) plus three standard deviations ($\sigma_{ROI}$) of the pixel values of the regions of interest was used as a threshold, which was subtracted from each image. WCIF Image J-W, version 1.43s (National Institutes of Health) was used to calculate the Manders overlap coefficients (R, M1 and M2), Pearsons Correlation Coefficient (r), and intensity correlation coefficient (ICQ). The Pearsons Correlation Coefficient was calculated as follows:

$$r = \frac{\sum(R_i - R_a) \times (G_i - G_a)}{\sqrt{\sum(R_i - R_a)^2 \times \sum(G_i - G_a)^2}} \qquad \textbf{Equation S-1}$$

where $R_i$ is red fluorescence intensity in pixel (i), $R_a$ is the average red fluorescence intensity, $G_i$ is green fluorescence intensity in pixel (i), $G_a$ is the average green fluorescence intensity. This coefficient measures the linear relationship between the intensities of two fluorophores on a pixel-by-pixel basis. Its range is from -1 to +1.

The Manders Overlap Coefficient (R) was calculated as follows:

$$R = \frac{\sum(R_i) \times (G_i)}{\sqrt{\sum(R_i)^2 \times \sum(G_i)^2}} \qquad \textbf{Equation S-2}$$

where the parameters are the same as those defined for the Pearson Correlation Coefficient. Its range is from 0 to +1.

The M2 Coefficient gives the number of green fluorescence pixels (GFP) that also register red fluorescence (AlexaFluor568) was calculated as follows:

$$M2 = \frac{\sum G_{i,coloc}}{\sum G_i} \qquad \textbf{Equation S-3}$$

where $G_{i,coloc}$ is the number of green fluorescence pixels with colocalized red fluorescence, and $G_i$ is the total number of pixels registering green fluorescence. Its range is from 0 to +1.

The ICQ was calculated as follows:

$$ICQ = \frac{\sum(R_i > R_a) = (G_i > G_a)}{N} - 0.5 \qquad \textbf{Equation S-4}$$

where the expression in the numerator refers to counting the number of pixels where both red ($R_i$) and green ($G_i$) fluorescence in pixel (i) are above or below their respective average, ($R_a$ and $G_a$), and N is the total number of pixels. The range of ICQ is from -0.5 to +0.5.

| **Table S-1**. Summary of colocalization analysis of GFP and Immunolabeling with a secondary antibody labeled with AlexaFluor 569 | | | | |
|---|---|---|---|---|
| | R | r | M2 | ICQ |
| Control (n=7) | 0.78 ± 0.08 | 0.50 ± 0.22 | 0.99 ± 0.01 | 0.23 ± 0.14 |
| Vinblastine-treated (n=6) | 0.84 ± 0.09 | 0.68 ± 0.14 | 0.97 ± 0.07 | 0.20 ± 0.13 |
| Rapamycin-treated (n=7) | 0.93 ± 0.04 | 0.80 ± 0.16 | 0.99 ± 0.01 | 0.30 ± 0.10 |

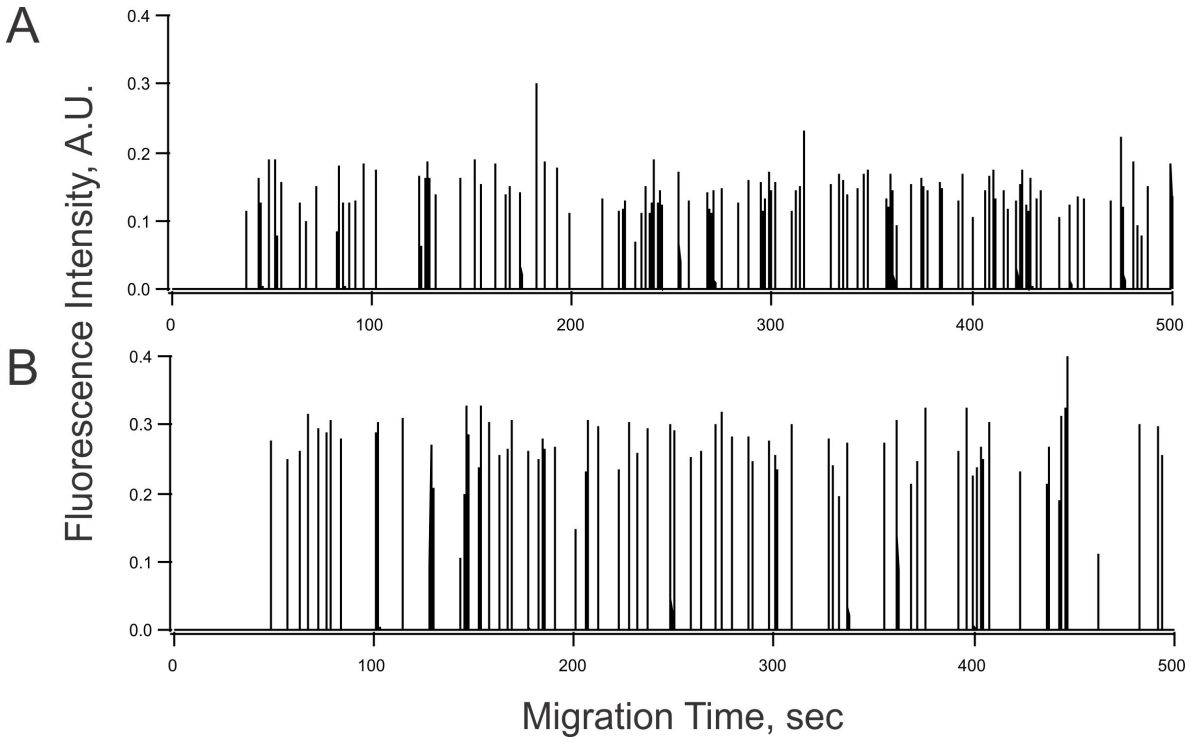


**Figure S-2.** Alignment of CE-LIF detector for individual organelle detection. (A) Bead Alignment using an applied electric field (-297 V/cm). (B) Bead Alignment using pressure-driven flow (10 psi). To confirm that 10 psi provided a linear flow of beads similar to the separation voltage used for autophagy organelle separation, (-300 V/cm), alignment with AlignFlow beads was done first by applying an electric field and then by using pressure-driven flow. AlignFlow beads were diluted in CE buffer (1% v/v) and continuously injected into the capillary using either approach. The %RSD of the AlignFlow beads was 13% and the average points per peak was 15 when using pressure-driven flow. The %RSD of the AlignFlow beads was 19% with 13 points per peak when using -297 V/cm. These values for -297 V/cm are comparable to values obtained with 10 psi. AlignFlow Beads first appeared after ~275 sec when using 10 psi. Using the pre-migration window for autophagosomes (450-500 sec), we can estimate the linear flow from voltage-based alignment and separations to be ~2-fold less when compared to the linear flow from pressure-based alignment. Based on the %RSD and points per peak shown here, this reduction in linear flow does not appear to significantly change the reproducibility of the detector.

| **Table S-2.** Alignment of CE-LIF detector prior to individual organelle detection | | | |
|---|---|---|---|
| Experiment | %RSD | Points Per Peak | n |
| Basal | 15 | 10 | 212 |
| Vinblastine | 13 | 15 | 154 |
| Rapamycin | 26 | 15 | 199 |
| Both Vinblastine and Rapamycin | 13 | 12 | 145 |

**S-3. Detector calibration and correction for variations in sensitivity and electrophoretic mobility.**

AlignFlow flow cytometry beads (Life Technologies, Grand Island, NY, 1:100 v:v in CE buffer) were used to align the PMT detector. (Figure S-2). All relative standard deviations determined for the AlignFlow beads were below or equal to 27%, which is the manufacturer's reported value (Table S-2).

Changes in detector sensitivity were determined to correct for changes in organelle GFP-LC3 levels as described in Section 4.6. In order to make this correction, we needed to confirm that the alignment was the main source of variation in detector sensitivity. We assumed that the background level was proportional to the instrument sensitivity. This assumption requires that standard deviation of the electropherogram background is proportional to the background level. When the ratios of standard deviation to background were compared they were consistent within 2-14% variation for the four different days when measurements were made. This difference suggests that the alignment of the custom-built instrument was the main cause for changing sensitivity. We used the background level of each run as the correction factor for variations in sensitivity.

While individual autophagy organelle fluorescence levels were corrected for differences in sensitivity of the fluorescence detector, detection of low-intensity autophagy organelle events such as phagophores and autolysosomes may not be detected in some electropherograms due to changes in limits of detection. This can cause some comparisons of organelle quantiles to be slightly skewed due to the inability to detect all individual organelles. The two treatments that were the most affected by this are the untreated and rapamycin-treated conditions. If we assume lower intensity events were not detected, detection of these low intensity events could lower the GFP-LC3-II values of all the percentile values (Figure 3). Overall, it is important to reiterate that when comparing percentiles of organelle events, these are comparisons of only the *detected* organelle events.

The reproducibility of the individual organelle fluorescence intensity and electrophoretic mobility distributions obtained from replicate CE-LIF separations of the same sample was assed using QQ plots. These plots confirmed that both properties had adequate reproducibility (Figure

S-3). Reproducible separations were pooled and used for comparisons of distributions of individual organelle GFP-LC3 fluorescence intensities and electrophoretic mobilities obtained under various conditions.

## S-4. Statistical Overlap Theory

When electropherograms have a large number of peaks, there is a probability that a single observed peak is composed of multiple events. The Statistical Overlap Theory uses the number of detected peaks ($m_{detected}$) in a bin to estimate the true number of events based on a probability of peak overlap. When $m_{detected}$ exceeds a critical saturation value ($m_{critical}$) predictions fail. In these studies, the CE-LIF trials were separated into different sections (bins) with a consistent number of seconds per bin (X), and the threshold saturation value (A) was estimated based on the peak width, X, and number of bins. Bins with a high probability of overlapped peaks (BWO) were detected when $m_{detected} > m_{critical}$. For BWO, we used $m_{critical}$ as a conservative estimate of the number of organelles present in that bin.

| **Table S-3.** Estimation of organelle events from observed peaks | | | |
|---|---|---|---|
| Basal autophagy, no vinblastine | Trial 1 | Trial 2 | Trial 3 |
| $m_{critical}$ | 152 | 100 | 98 |
| A | 0.13 | 0.17 | 0.17 |
| X | 97 | 67 | 77 |
| Bins | 12 | 14 | 14 |
| BWO | 0 | 3 | 5 |
| $m_{detected}$ | | 128, 135, 230, | 117, 167, 123, 140, 157 |
| Basal autopahgy, vinblastine | Trial 1 | Trial 2 | Trial 3 |
| $m_{critical}$ | 197 | 182 | 196 |
| α | 0.11 | 0.11 | 0.11 |
| X | 87.4 | 77.3 | 86.6 |
| Bins | 15 | 20 | 17 |
| BWO | 3 | 7 | 5 |
| $m_{detected}$ | 322, 321, 235 | 299, 831, 683, 414, 430, 278, 464 | 274, 364, 298, 258, 294 |
| Rapamycin-enhanced autophagy, no vinblastine | Trial 1 | Trial 2 | Trial 3 |
| $m_{critical}$ | 251 | 284 | 281 |
| α | 0.09 | 0.09 | 0.09 |
| X | 107.6 | 104.6 | 128.1 |
| Bins | 15 | 17 | 16 |
| BWO | 2 | 3 | 1 |
| $m_{detected}$ | 399, 389 | 553, 684, 324 | 473 |

| Rapamycin-enhanced autophagy, Vinblastine | Trial 1 | Trial 2 | Trial 3 |
|---|---|---|---|
| $m_{critical}$ | 254 | 277 | 284 |
| α | 0.09 | 0.09 | 0.09 |
| X | 109.4 | 125.6 | 130.1 |
| Bins | 13 | 14 | 10 |
| BWO | 0 | 1 | 0 |
| $m_{detected}$ | | 286 | |

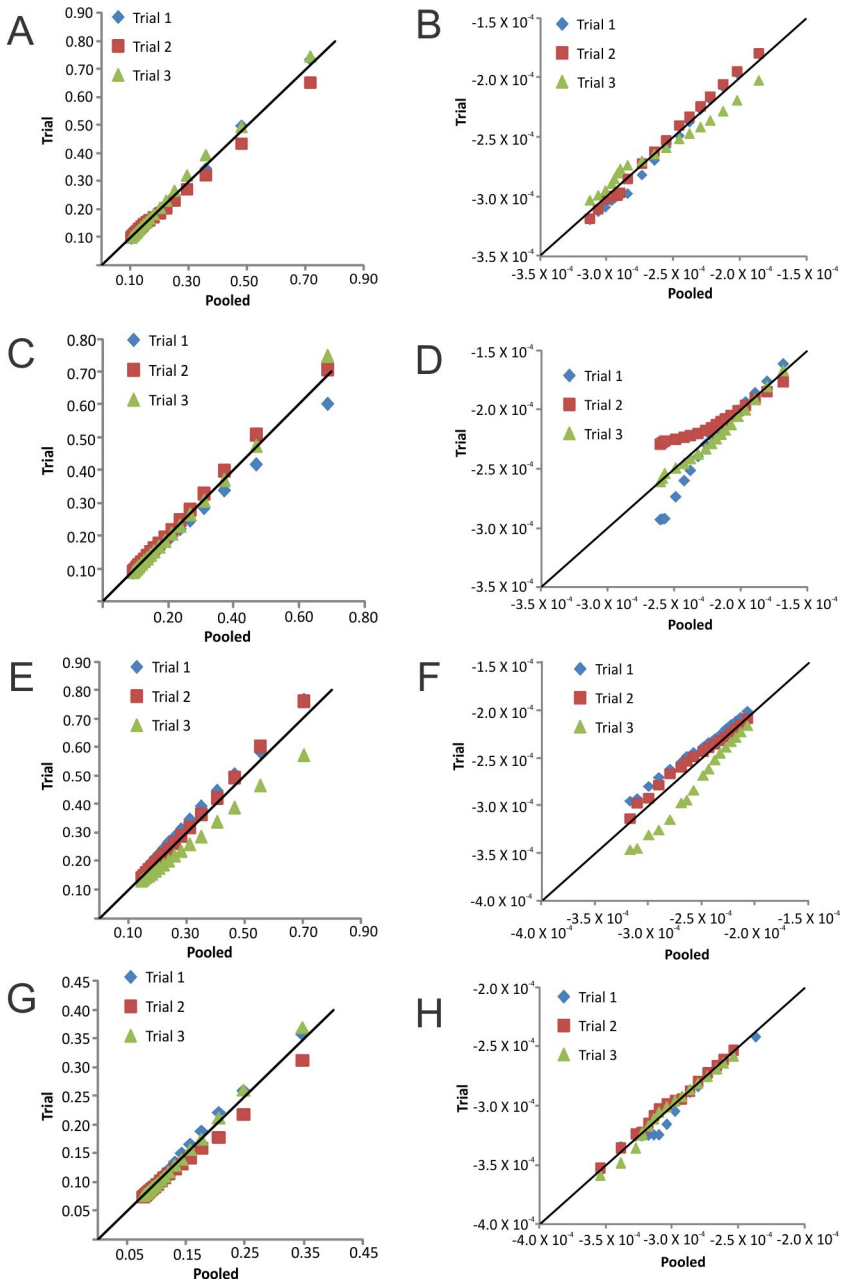


**Figure S-3.** QQ plots of each replicate (y-axis) versus the pooled data (x-axis). (A) GFP-LC3 fluorescence intensity, basal autophagy. (B) Electrophoretic mobility, basal autophagy. (C) GFP-LC3 fluorescence intensity, basal autophagy and vinblastine treatment. (D): Electrophoretic mobility, basal autophagy and vinblastine treatment. (E): GFP-LC3 fluorescence intensity, rapamycin-enhanced autophagy. (F) Electrophoretic mobility, rapamycin-enhanced autophagy. (G): GFP-LC3 fluorescence intensity, rapamycin-enhanced autophagy and vinblastine treatment. (H): Electrophoretic mobility, rapamycin-enhanced autophagy and vinblastine treatment.

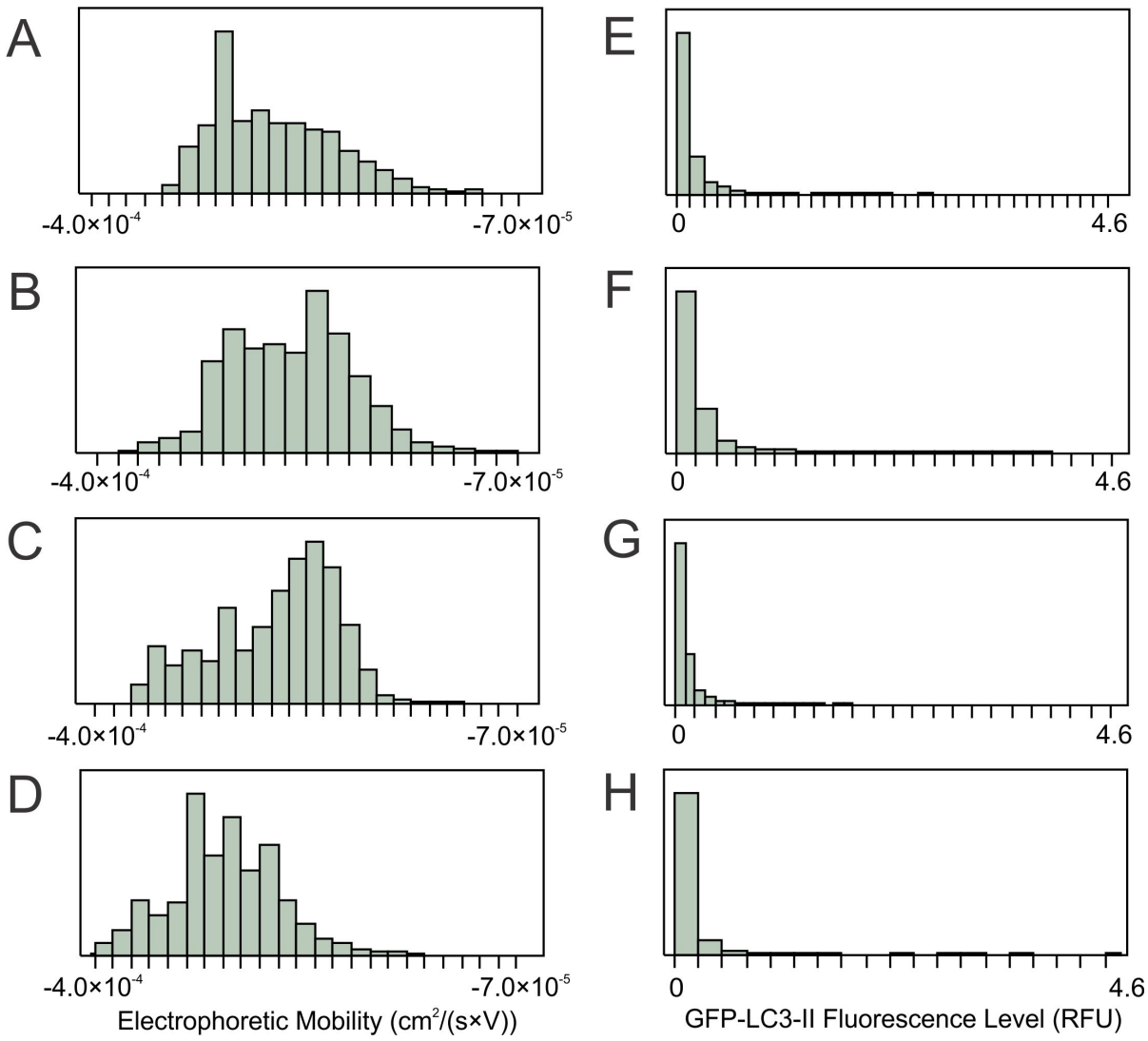


**Figure S-4.** Distributions of electrophoretic mobility and of GFP-LC3-II fluorescence levels for individual autophagy organelle values. (A) Basal autophagy electrophoretic mobility. (B) Basal autophagy after vinblastine treatment electrophoretic mobility. (C) Rapamycin enhanced autophagy electrophoretic mobility. (D) Rapamycin enhanced autophagy after vinblastine treatment electrophoretic mobility. (E) Basal autophagy GFP-LC3-II fluorescence levels. (F) Basal autophagy after vinblastine treatment GFP-LC3-II fluorescence levels. (G) Rapamycin enhanced autophagy GFP-LC3-II fluorescence levels. (H) Rapamycin enhanced autophagy after vinblastine treatment GFP-LC3-II fluorescence levels. Each set of data was divided into 18 columns, based on the lowest number of data points of the four conditions. R.F.U. = relative fluorescence units.

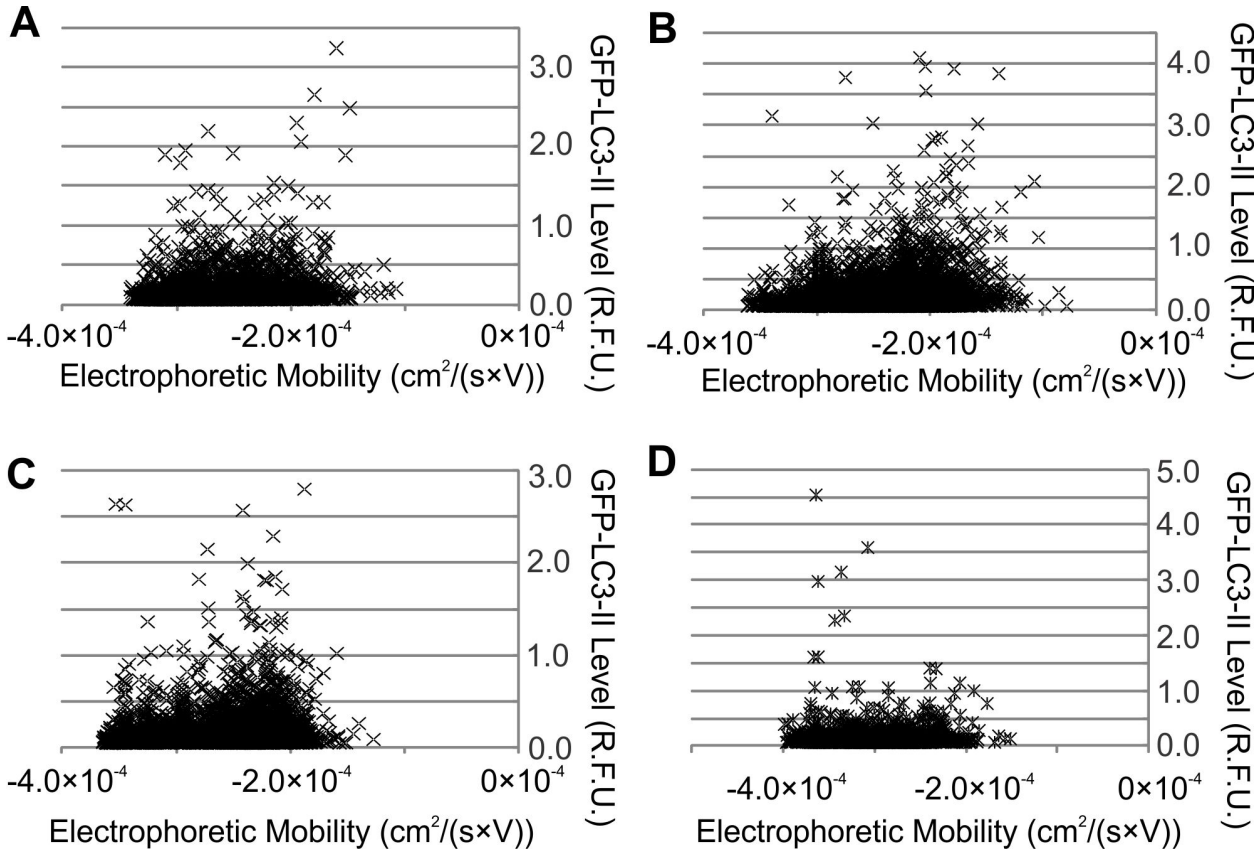


**Figure S-5.** Comparison of GFP-LC3-II fluorescence levels and electrophoretic mobility of autophagy organelles. (A) Basal autophagy. (B) Basal autophagy after vinblastine treatment. (C) Rapamycin enhanced autophagy. (D) Rapamycin enhanced autophagy after vinblastine treatment. R.F.U. = relative fluorescence units.